Eur. Phys. J. D (2021) 75:264
https://doi.org/10.1140/epjd/s10053-021-00247-9

THE EUROPEAN PHYSICAL JOURNAL D

Regular Article – Atomic and Molecular Collisions

Electron collision with N_2H and HCO

Paresh Modak[1], Abhisek Singh[2], Biplab Goswami[3], and Bobby Antony[1,a]

[1] Atomic and Molecular Physics Lab, Department of Physics, Indian Institute of Technology (Indian School of Mines), Dhanbad 826004, India
[2] RP & AD, BARC, Mumbai, India
[3] Gaya College of Engineering, Srikrishna Nagar, Khizarsarai, Bihar 823003, India

Received 15 May 2021 / Accepted 12 August 2021 / Published online 5 October 2021

Abstract. The elastic and excitation processes for e-N_2H/HCO systems are investigated in this article. The calculations are performed within the framework of R-matrix theory implemented using the pseudo-state formalism. Electron attachment to N_2H/HCO during electron collision is found to produce temporary negative ion states. We observed two negative ion states, X^1A' and $^3A''$, in the elastic scattering channel for the present targets. The generation of negative ions in the inelastic (electronic excitation) channel is also observed. Formation of H^- ion is traced out by investigating the dissociative electron attachment process for the e-N_2H/HCO scattering system. A detailed investigation of the elastic and electronic excitation processes of e-N_2H/HCO systems is reported here. The results presented here will be key to understand various intermediate processes occurring in N_2H- and HCO-rich environments.

1 Introduction

N_2H has an important role in atmospheric nitrogen production. This molecule is the intermediate of diimide formation through various processes, viz. oxidation of hydrazine [1,2], thermal cycloreversion of diimide-anthracene adduct [3], hydrolysis of azodicarboxylic acid [1,2,4,5], pyrolysis of p-toluenesulfonylhydrazine [5], and microwave discharge decomposition of hydrazine [6]. N_2H has a decisive role in the production of low-temperature ammonia synthesis [7] too. Studies related to geometry and structure of N_2H in the ground and excited states are found in the literature. However, no investigation on scattering processes for the e-N_2H system is available to the best of our knowledge. Vasudevan et al. [8] studied ground and excited states of N_2H using *ab initio* SCF and CI methods. Baird et al. [9] also reported *ab initio* molecular orbital calculations for the ground and lowest-lying excited states. Pasto et al. [10] reported the energy and optimized geometry of N_2H using SCF method, while Qian et al. [11] reported its stoichiometry and structure. The instability ($10^{-9}-10^{-12}$ s) [12] of neutral N_2H at ground state is the main reason for the lack of e-N_2H experimental data. HCO is an open-shell species and is an important intermediate to many environments viz. combustion of hydrocarbons, photolytic decomposition of formaldehyde and higher aldehydes, and polluted atmospheres [13]. It's an important precursor for the formation of O-bearing complex organic and prebiotic molecules [14]. It is assumed to be at the onset of the formation of glycolaldehyde (CH_2OHCHO) upon ice surfaces via HCO dimerization followed by successive hydrogenations [15]. HCO is a tracer of regions where active photochemistry is induced by far-ultraviolet radiation [16]. It is also observed in cold dark clouds [17,18] and in the Horsehead Nebula [16,19]. The first spectroscopic studies of this molecule are from Ramsay [20] and Herzberg and Ramsay [21] using flash photolysis method. Later the excited-state potential surfaces were reported by Larson et al. [22]. Its electronic spectrum was studied by ESR [23] and infrared spectroscopy [24] in a low-temperature solid matrix. Furthermore, electron collision with N_2H and HCO can produce anionic bound states, N_2H^- and HCO^-, which are dissociative in nature. Earlier Francois et al. [25] has proposed a unique bound asymptote (H^- and N_2) of N_2H^-. Stoecklin et al. [26] calculated radiative association cross section for N_2 and H^- and predicted existence of N_2H^-. Stoecklin et al. [27] also reported formation of HCO^- ion through radiative association of H^- and CO, and radiative electron attachment to HCO. The dissociation of N_2H^-/HCO^- ends up forming neutral N_2, H, CO, and H^- ions. Furthermore, collision of N_2H^- with neutral H_2 can generate H^- ion at room temperature [25]. The H^- ion has key role in the chemistry of various astrophysical environments [28,29]. Experimental studies of the anion in gas phase remain a challenge to-date. Therefore, theoretical studies of negative bound state during electron collision could shine light in this case. Information on negative ion formation pathway is essential to probe the relevant chemistry and hence the electron

[a] e-mail: bobby@iitism.ac.in (corresponding author)

scattering data. The formation of N_2H^{-*} and HCO^{-*} is very unstable. Therefore, comprehensive knowledge of e-N_2H/HCO bound system will provide the crucial information on: (1) the correct dissociative electron attachment channel, which will help to study formation of H^- ion from e-N_2H/HCO system, and (2) the asymptotic bound state of N_2H^-/HCO^-, which has dynamical consequences in ionospheric chemistry.

In the present endeavor, we investigated the formation of negative bound states through elastic and electronic excitation channels for e-N_2H/HCO collision systems. The dissociative electron attachment (DEA) process is also studied to trace the formation of H^- ion during electron scattering from the present isoelectronic systems. We employed the *ab initio* R-matrix method [30–32] for the present calculations. The codes were implemented through the Quantemol N expert system [33]. The R-matrix can include the correlation effects adequately and give a fair description of excited states of the molecule. For the present calculation, we used static-exchange (SE) and complete active space-configuration interaction (CAS-CI) models. The incoming electron can occupy one of the excited orbitals of the target during scattering and such processes end up forming negative molecular ion for a finite time causing resonances.

2 Method

2.1 General methodology

The basic idea of the R-matrix theory is to divide the configuration space into two regions by a sphere of radius a, centered on the center of mass of the target molecule (Fig. 1).

The inner region contains both the scattering and target electrons. Hence short-range potentials, viz. exchange and correlation are dominant. Outside the sphere, only the long-range multipolar interactions are considered; thus scattering electron is free in the outer region and the problem converges to a simple free particle problem. Therefore, the correct choice of R-matrix radius is very important such that target wave function and short-range potentials must vanish at the boundary surface.

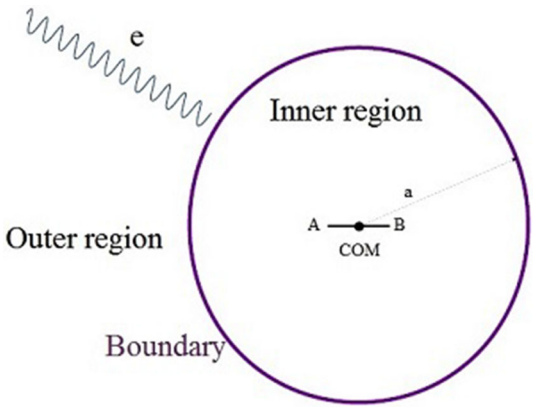

Fig. 1 Schematic diagram for the R-matrix method. a is the radius of R-matrix sphere and COM represents the center of mass of the molecular system, AB

The inner region wave function is expressed as a sum of continuous and target wave functions:

$$\Psi_k = \mathcal{A}\sum_{ij}\Phi_i(x_1,....,x_N)u_{ij}(x_{N+1})a_{ijk} + \sum_i b_i\chi_i \tag{1}$$

where '$\mathcal{A}$' is anti-symmetrization operator, $u_{ij}(x)$ are the continuum orbitals of the target and Φ_i are the target wave functions. For the SE model, Φ_i are constructed using HF orbitals, whereas for CAS-CI model Φ_i are generated considering valence electrons as active. The χ_i are two-center quadratically integrable (L^2) functions. These functions are used to model the target polarization and correlation. The solutions of the inner region Hamiltonian are used to set up the R-matrix at the boundary of the sphere. These are then propagated to the asymptotic region (a_{out}), where matching is done with the asymptotic functions obtained from the Gailitis expansion [34].

2.2 Dissociative electron attachment

In this article, the formation of H^- ion is predicted investigating the dissociative electron attachment (DEA) process during e-N_2H/HCO scattering. The cross section for the DEA process has been calculated using the information of bound states viz. resonance cross section and survival probability of a bound state, that appears in elastic and electronic excitation processes. The DEA cross section for a polyatomic system can be expressed as:

$$\sigma_T(E) = C\sum_i S_i\sigma_{ri}(E) \tag{2}$$

where E is the incident electron energy and i is the number of resonances below the IP of the target. σ_{ri} and S_i are resonance cross section and survival probability of the resonant state i, respectively. The coefficient C is a compensating factor and is fixed as 0.7 [35]. σ_r are computed using the resonance energies and widths, whereas S_i are computed using target and resonance potentials [35]. The required quantities are the H-N_2/H-CO bond dissociation energy, D_e and ground state vibrational energy, E_v of the target molecule, and electron affinity, E_a of the dissociating fragment, H. The resonance position, E_r and width, Γ_i are computed using the RESON program [36], which uses the Breit–Wigner formula to fit the eigenphase sum. The details of the procedure are given by Munro et al. [35].

N_2H and HCO are open-shell radicals having a high value of permanent dipole moments. The quality of

wave function for such a target depends on an accurate description of polarizability, dipole moment, and channel coupling effect. We first employed SE model for the ground state of N_2H/HCO and then performed CAS-CI calculations using occupied and virtual molecular orbitals. The target geometries were obtained from cccbdb database [37]. All calculations were performed in the ground state of N_2H/HCO with bend geometry, where the target was placed in the xy plane (C_s point group). The ground state configuration in bend geometry of the present targets is $(1a')^2, (2a')^2, (3a')^2, (4a')^2, (5a')^2, (6a')^2, (1a'')^2, (7a')^1$. cc-pVDZ basis was used for the target description in the present study. For the SE model, all electrons were frozen, whereas for CAS-CI calculation orbitals [1-4a′]^8 was frozen and a CAS of [5-9a′,1-2a″]^7 was included. The present method uses first-order perturbation theory to model target polarization. Only single excitations were considered in the present study. R-matrix radius of 10 a_0 was chosen to enclose the charge cloud of the target molecule.

2.3 Calculation

In the SE model three unoccupied or virtual orbitals (2 for A' symmetry and 1 for A'' symmetry) are included in the L^2 configurations, which is obtained by placing the scattering electron in these virtual target orbitals. The final calculations were made by employing the CAS-CI method. To preserve the correlation effect, we have frozen 8 inner electrons and the 7 outer electrons (valence electrons) were placed in active space. Also, 2 orbitals of A' and 1 orbital of A'' symmetry were augmented over valence orbital to the active space. This produces 108 configuration state functions (CSFs) and gives a fair description of N_2H/HCO at all internuclear distances. The values obtained for the ground state energy, dipole moment, and rotational constant for the present targets are reported in Table 1 with previous available data [37]. The deviation of present calculated values from previously reported data is also presented here. The value of dipole moment is slightly lower, however an overall good agreement has been obtained for the target properties. Calculations were performed for the $^1A'$, $^3A'$, $^1A''$, and $^3A''$ scattering symmetries for the ground state of N_2H/HCO radicals. 25 virtual orbitals (8-24a′, 2-9a″) were included in the present calculation to obtain a converged target wave function. These virtual orbitals were also used to model the target polarizability. The K matrices were constructed using 28 target states and 115 scattering channels from the molecular orbitals. The T-matrices were then calculated from the K matrices. The contributions from $l \leq 4$ were explicitly incorporated in the present work and higher partial waves ($4 < l \leq 6$) were included through Born correction [38,39]. The continuum orbitals were orthogonalized to the target orbitals (Eq. 1) and overlap of less than 2×10^{-8} was removed to resolve the linear dependence [31]. N_2H/HCO has a permanent dipole moment of 2.177 D/1.837 D [37], respectively. This value was used in calculating long-range dipole interaction in the outer region, since the present calculated values of dipole moment are lower (Table 1). The outer region wave function was then propagated to large distances (a_{out} = 100 a_0) [32] for the fulfillment of asymptotic condition. The values of target properties reported in Table 1 are used for the final calculation.

Table 1 Values of target properties with percentage deviation

Target	Target property	Present	cccbdb [37]
N_2H	Ground state energy	−109.471	−109.996
	Dipole moment	1.956	2.122
	Rotational constant	21.721	22.306
HCO	Ground state energy	−113.285	−113.817
	Dipole moment	1.679	1.837
	Rotational constant	22.708	22.365

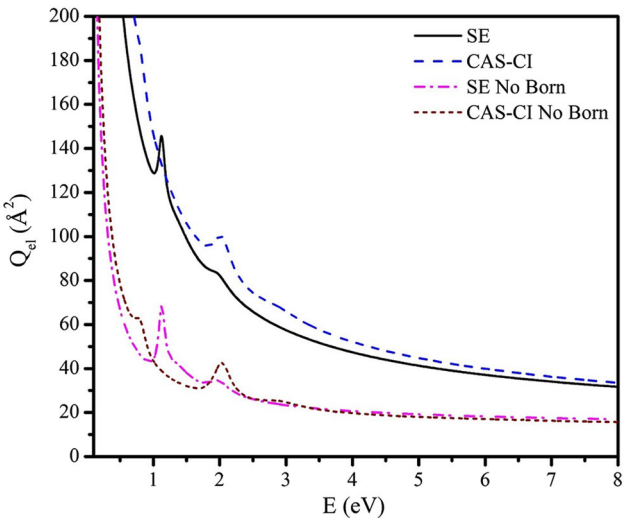

Fig. 2 Elastic cross section for e-N_2H scattering

3 Results and discussion

The results of the present calculations are presented in this section for a fine energy grid of 0.02 eV to resolve fine structures. The resonances are studied using eigenphase sum (not shown here) of a particular symmetry, and bound states are identified using the Breit–Wigner fitting formula [36].

3.1 Elastic cross section

Figure 2 represents elastic cross section (Q_{el}) for N_2H. The presence of strong dipole moment intensifies electron scattering in the forward direction and diverges the cross section below 1 eV. The effect of target polarization has been fairly described using the R-matrix

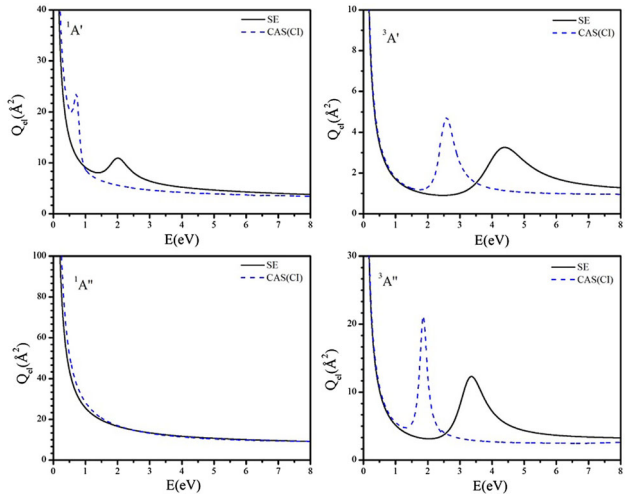

Fig. 3 Elastic cross section for e-N_2H/HCO scattering

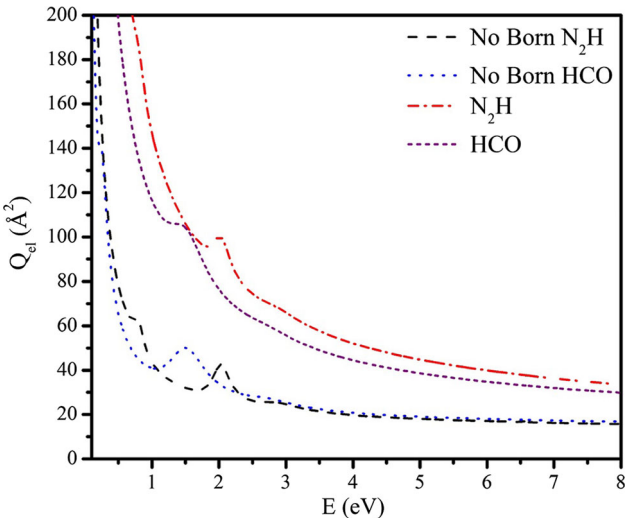

Fig. 4 Elastic cross section for e-N_2H/HCO scattering

pseudo-states (RMPS) method in our final calculation. The polarization potential is the key parameter in detecting the resonances and calculating its parameters. The correlation effect lowers the energy of target states resulting in a shift in the bound states toward the low energy side. Also a slight increase in the magnitude of Q_{el} is observed for slow electrons due to exchange-correlation, which is very dominant in that region. Consideration of $l > 4$ intensifies the long-range interaction and leads to a significant change in the cross section value. The difference in magnitude between the total elastic cross sections calculated employing SE and CAS-CI models are quite small due to the presence of repulsive states, which has leading contribution in total elastic curve. However, in case of the partial elastic curve (Fig. 3), we observe significant difference in the cross section between these models. For HCO, we obtained a similar nature and shape of the elastic scattering curve and the reason for this behavior is same as that of

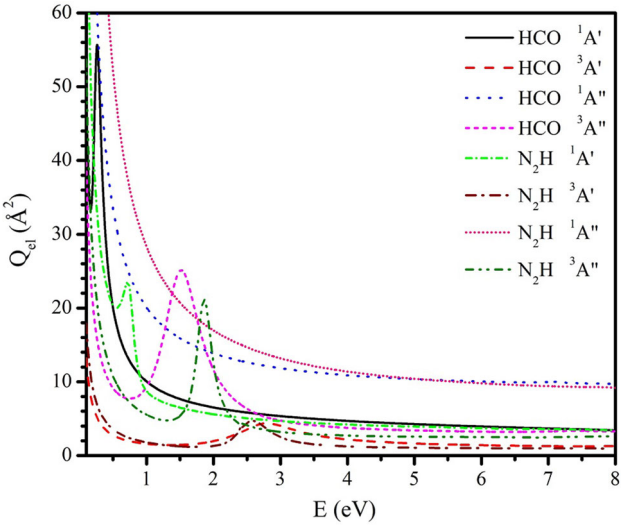

Fig. 5 Partial elastic cross section for e-N_2H/HCO scattering. Solid: HCO $^1A'$; Dash: HCO $^3A'$; Dot: $^1A''$; Short Dash: $^3A''$; Short Dash Dot: N_2H $^1A'$; Dash Dot: $^3A'$; Short Dot: $^1A''$; Dash Dot Dot: $^3A''$

its isoelectric counterpart. Therefore, we used the final results of e-HCO for comparison purposes.

Figure 4 shows a comparative view of the elastic cross section for e-N_2H and e-HCO systems. The bond angle of HCO is higher than N_2H molecule, which reflects in its elastic cross section. Born correction further magnifies the effect of compact structure for e-N_2H scattering. Three bound state-like structures were obtained for both the targets. These structures indicate formation of the anionic states for the e-N_2H/HCO system. The shifting in resonance position is due to the electron affinity of different constituents.

3.2 Partial cross section

The partial cross section for each scattering symmetry is reported in Fig. 5. The resonances, which were superficial in the Q_{el}, appear prominently here for the respective symmetries. The partial cross sections will help to identify the correct scattering channel responsible for the formation of different resonant states. Two scattering channels are identified forming two resonant states corresponding to $^1A'$ and $^3A''$ symmetries. These resonances appear due to electron confinement onto 7a′, and 2a″ orbitals of present isoelectronic systems. The resonance-like structure corresponds to ^{3}A′ symmetry is due to the local rise in the eigenphase curve of same symmetry. As discussed above, there is a shift in the resonance position of the two isoelectronic systems due to differences in electron affinity of different dissociative products. The configuration for these temporary bound states is reported in Table 2 with resonance energy. All the resonances are shape resonances. The resonances detected in the present study support the prediction of N_2H^- complex of Francois et al. [25].

Table 2 Anionic states of N_2H & HCO

State	Configuration	Resonance Energy (eV)		Resonance Width (eV)	
		N_2H	HCO	N_2H	HCO
X^1A'	$[(1a'')^2\ (7a')](7a')$	0.787	0.244	0.217	0.132
$^3A''$	$[(1a'')^2\ (7a')^1\ ](2a'')$	1.841	1.483	0.270	0.667
$^3A'$	$[(4a')(5a')^2(6a')^2$ $(1a'')(7a')](2a'')$	7.856	7.085	0.315	0.378

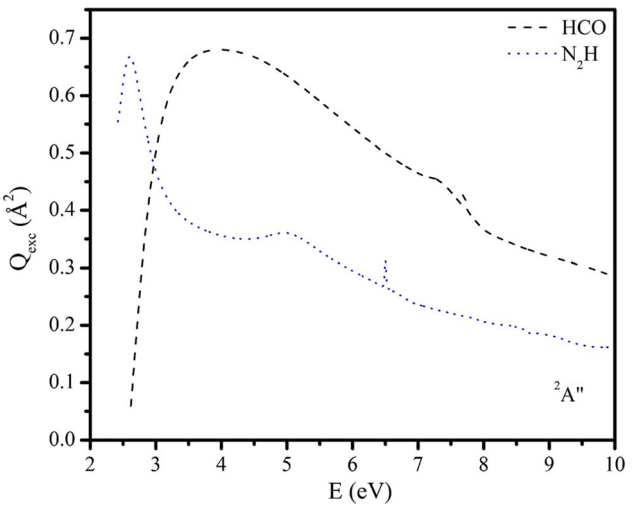

Fig. 6 Excitation cross section for $^2A'' \leftarrow X^1A'$ transition of N_2H/HCO

3.3 Excitation cross section

The excitation cross section for $^2A'' \leftarrow X^2A'$ transition is represented in Fig. 6. The value of excitation threshold obtained for this state is 0.40 eV higher than the experimental result [40]. The $^2A''$ state is the ground state in linear geometry. This is the reason for high value of cross section for the transition to this state. A steady increase in the cross section was observed for both targets, just above the excitation threshold.

For N_2H, a resonance like structure has been identified for the $^2A'' \leftarrow X^2A'$ transition. This results from a steady rise in the eigenphase curve of $^1A''$ and $^3A''$ at 2.60 eV. A broad structure is observed for HCO, which corresponds to the local rise in eigenphase near 2.80 eV for the singlet and triplet states of A″ symmetry. Shoulder like structures are also seen near 5 eV & 7 eV for N2H & HCO, respectively, primarily due to the irregular nature of the eigenphase curve of A″ symmetry. The second dipole allowed transition (Fig. 7), $8a' \leftarrow 7a'$ is Rydberg like. The cross section for this transition increases smoothly and has the second-highest contribution in the excitation process for N_2H. For HCO, bound state-like structures arise due to increase in eigenphase of A′ symmetry. The cross section for transition to $^3A'$ and $^3A''$ is shown in Fig. 8. These states also show a steady increase in cross section. Feshbach resonance has been observed for the $^3A'$ state,

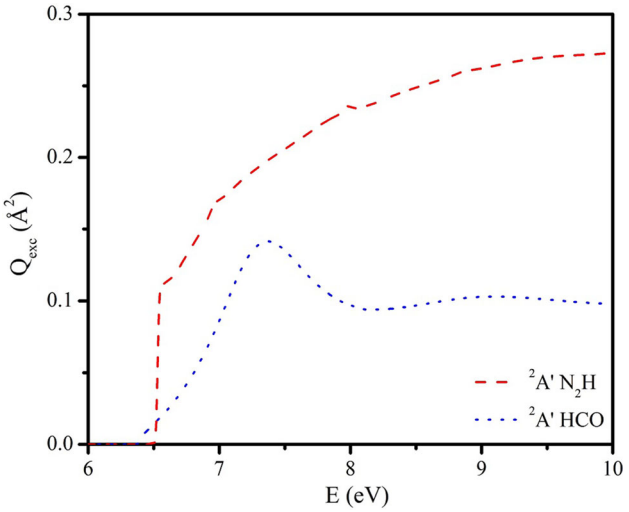

Fig. 7 Excitation cross section for $^2A' \leftarrow X^1A'$ transition

while for $^3A''$ state resonance like structure has also been obtained due to the local rise in eigenphase sum curve. The resonance configurations of these excited states are reported in Table 2. Cross section corresponding to other transitions are negligible compared to the one presented here.

3.4 Dissociative electron attachment cross section and formation of H^- ion

In Fig. 9, we report cross section for the dissociative electron attachment (DEA) process during electron scattering from N_2H/HCO molecular system. We observed two DEA peaks around 1.97 eV and 6.89 eV. The first peak corresponds to dissociation channel associated with the $^3A''$ state. The second peak is much higher and arises through Feshbach resonance.

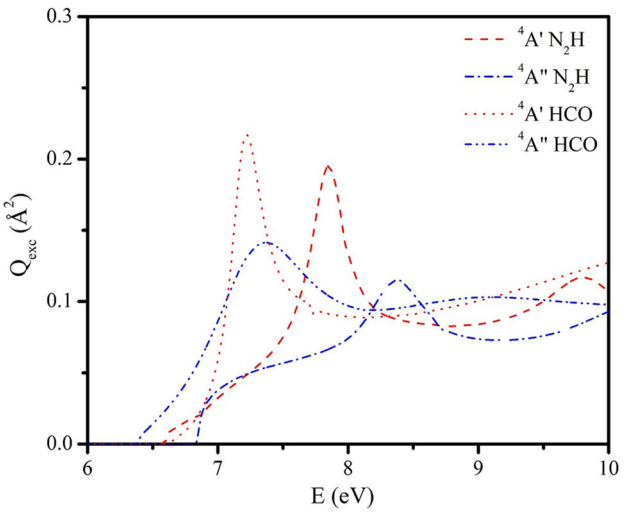

Fig. 8 Cross section for transition to bent states of N_2H/HCO

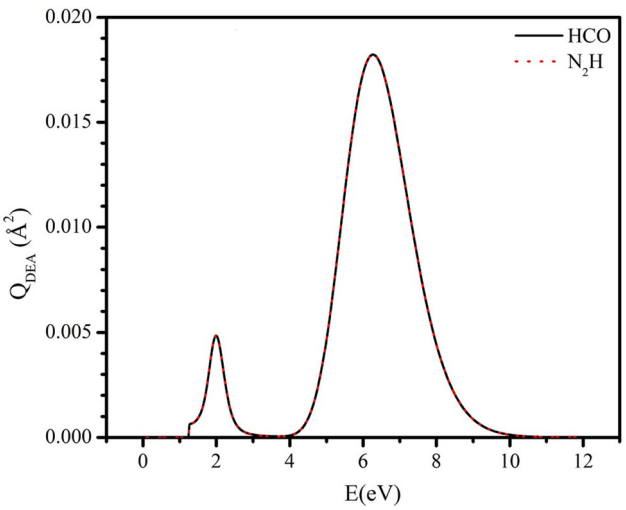

Fig. 9 Dissociative electron attachment cross section for e-N_2H/HCO scattering

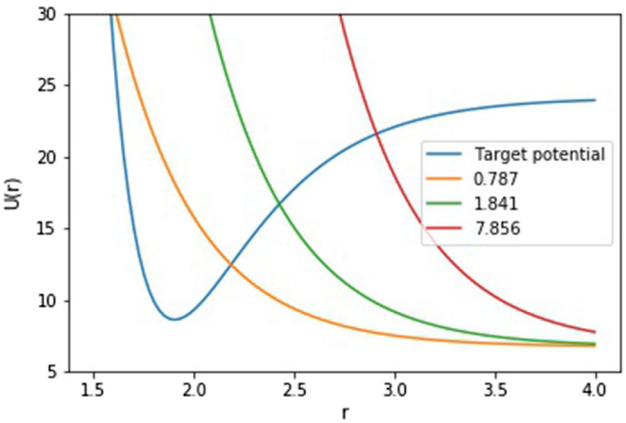

Fig. 10 Model potential used for DEA study for N_2H. For HCO, the nature and shape of the potential are same

The model potentials [35] used to study the DEA process are shown in Fig. 10 for different resonance widths. The intersections represent the radial distance at which the target dissociates before autoionization. The resonance configuration for these states is shown in Table 2.

4 Conclusion

We investigated elastic and electronic excitation processes for e-N_2H/HCO collision systems. The scattering processes were studied using the CAS-CI model and a comprehensive description of scattering cross sections is reported. Asymptotic behavior was observed for the elastic cross sections due to strong dipole potential below 1 eV. Results were analyzed and two resonant states were found for the molecular targets. Partial channels were analyzed to obtain the correct pathway for formation of these anionic states. The present study identifies the attractive potential for three scattering states, $^1A'$, $^3A'$ and $^3A''$ and repulsive potential for $^1A''$ diverging state. Present study confirmed earlier prediction [25–27] of asymptotic bound states of N_2H^-/HCO^-.

The excitation processes are studied and resonances are characterized using the eigenphase diagram. Both targets permit resonances in excited states. These are Feshbach type and no core excitation is obtained in the present case.

Formation of H^- ion was observed investigating the DEA channel for e-N_2H/HCO system. The two resonant states, $^3A''$ and $^4A'$, dissociate to form H^- ion. This is the first report on electron scattering from N_2H and HCO which supports the formation of H^- through dissociative electron attachment from N_2H/HCO. In conclusion, the present study support the earlier prediction of the formation of N_2H^-/HCO^- complex and H^- ion. Thus, the present results will reveal key information for various intermediate processes occurring in N_2H- and HCO-rich environments.

Acknowledgements BA acknowledges the support by SERB, Govt. of India through project Grant No. EMR/2016/005035 and BG acknowledges the support by TEQIP Collaborative Research Scheme with CRS ID:1-5728112461 for this research. The authors also acknowledge the valuable suggestions from Dr. Suvam Singh during preparation of the manuscript.

Author contributions

P.M. and B.A. conceived of the presented idea. P.M. performed the computations. A.S. assisted with calculations. B.A. supervised the work. All authors discussed the results and contributed to the final manuscript.

Data availability statement This manuscript has no associated data, or the data will not be deposited. [Author's comment: The datasets generated during and/or analysed during the current study are available from the corresponding author on reasonable request.]

References

1. E. Corey, W. Mock, D. Pasto, Tetrahedron Letters **2**, 347 (1961)
2. S. Hünig, H.R. Müller, W. Thier, Tetrahedron Letters **2**, 353 (1961)
3. E.J. Corey, W.L. Mock, Journal of the American Chemical Society **84**, 685 (1962)
4. R.S. Dewey, E.E. van Tamelen, Journal of the American Chemical Society **83**, 3729 (1961)
5. E.E. van Tamelen, R.S. Dewey, R.J. Timmons, Journal of the American Chemical Society **83**, 3725 (1961)
6. C. Willis, R.A. Back, Canadian Journal of Chemistry **51**, 3605 (1973)

7. K. Murakami, Y. Tanaka, R. Sakai, K. Toko, K. Ito, A. Ishikawa, T. Higo, T. Yabe, S. Ogo, M. Ikeda et al., Catalysis Today **351**, 119 (2020), sI:Sydney Catal Symposium18
8. K. Vasudevan, S. Peyerimhoff, R. Buenker, Journal of Molecular Structure **29**, 285 (1975)
9. N.C. Baird, H.B. Kathpal, Canadian Journal of Chemistry **55**, 863 (1977)
10. D.J. Pasto, D.M. Chipman, Journal of the American Chemical Society **101**, 2290 (1979)
11. E.J. Corey, W.L. Mock, D.J. Pasto, Scientific Reports **6**, 1 (2016)
12. S.F. Selgren, P.W. McLoughlin, G.I. Gellene, The Journal of Chemical Physics **90**, 1624 (1989)
13. van Mourik Tanja, D.T. H., P.K. A., The Journal of Physical Chemistry A **104**, 2287 (2000)
14. A.J. Ocaña, E. Jiménez, B. Ballesteros, A. Canosa, M. Antiñolo, J. Albaladejo, M. Agúndez, J. Cernicharo, A. Zanchet, P. del Mazo et al., The Astrophysical Journal **850**, 28 (2017)
15. P.M. Woods, B. Slater, Z. Raza, S. Viti, W.A. Brown, D.J. Burke, Astrophysical Journal **777**, 90 (2013). arXiv:1309.1164
16. M. Gerin, J.R. Goicoechea, J. Pety, P. Hily-Blant, Astronomy and Astrophysics **494**, 977 (2009)
17. J. Cernicharo, N. Marcelino, E. Roueff, M. Gerin, A. Jiménez-Escobar, G.M.M. Caro, The Astrophysical Journal **759**, L43 (2012)
18. A. Bacmann, A. Faure, Astronomy and Astrphysics **587**, A130 (2016)
19. V. Guzmán, J. Pety, J.R. Goicoechea, M. Gerin, E. Roueff, Astron. Astrophys. **534**, A49 (2011)
20. D.A. Ramsay, The Journal of Chemical Physics **21**, 960 (1953)
21. H. G, D.A. Ramsay, Proceedings of the Royal Society **233**, 34 (1955)
22. A. Larson, S. Tonzani, R. Santra, C.H. Greene, Journal of Physics: Conference Series **4**, 148 (2005)
23. F.J. Adrian, E.L. Cochran, V.A. Bowers, The Journal of Chemical Physics **36**, 1661 (1962)
24. G.E. Ewing, W.E. Thompson, G.C. Pimentel, The Journal of Chemical Physics **32**, 927 (1960)
25. L. Francois, H. Philippe, S. Thierry, H. Majdi, The Journal of Chemical Physics **136**, 244302 (2012)
26. T. Stoecklin, F. Lique, M. Hochlaf, Phys. Chem. Chem. Phys. **15**, 13818 (2013)
27. T. Stoecklin, P. Halvick, M. Lara-Moreno, T. Trabelsi, M. Hochlaf, Faraday Discuss. **212**, 101 (2018)
28. J.H. Black, The Astrophysical Journal **222**, 125 (1978)
29. D. Field, Astronomy and Astrophysics **362**, 774 (2000)
30. P.G. Burke, J. Tennyson, Molecular Physics **103**, 2537 (2005)
31. L.A. Morgan, C.J. Gillan, J. Tennyson, X. Chen, Journal of Physics B: Atomic, Molecular and Optical Physics **30**, 4087 (1997)
32. J. Tennyson, Physics Reports **491**, 29 (2010)
33. J. Tennyson, D.B. Brown, J.J. Munro, I. Rozum, H.N. Varambhia, N. Vinci, Journal of Physics: Conference Series **86**, 012001 (2007)
34. M. Gailitis, Journal of Physics B: Atomic and Molecular Physics **9**, 843 (1976)
35. J.J. Munro, S. Harrison, M.M. Fujimoto, J. Tennyson, Journal of Physics: Conference Series **388**, 012013 (2012)
36. J. Tennyson, C.J. Noble, Computer Physics Communications **33**, 421 (1984)
37. https://cccbdb.nist.gov
38. H. Munjal, K.L. Baluja, J. Tennyson, Phys. Rev. A **79**, 032712 (2009)
39. N. Sanna, F. Gianturco, Computer Physics Communications **114**, 142 (1998)
40. J.W.C. Johns, S.H. Priddle, D.A. Ramsay, Discuss. Faraday Soc. **35**, 90 (1963)